EXPLORING EMPLACEMENT MECHANISMS FOR PHYLLOSILICATE OUTCROPS IN WEST MARGARITIFER TERRA, MARS. K. D. Seelos[1], R. E. Maxwell[2,1], F. P. Seelos[1], D L. Buczkowski[1], and C. E. Viviano-Beck[1], [1]JHU Applied Physics Laboratory, Laurel, MD (kim.seelos@jhuapl.edu); [2]Dept. of Earth and Planetary Sciences, UCSC, Santa Cruz, CA.

Introduction: Clay minerals found in stratigraphic sequences have been used to support the idea of widespread precipitation and pedogenic weathering during a warmer, wetter climate era on early Mars [e.g. 1-2]. These sequences have been identified in several provinces, including along the walls and on the plains surrounding/south of Valles Marineris [3-5], in Mawrth Vallis [1,6], Meridiani [2,7-8], and Nili Fossae [9], where Fe/Mg phyllosilicates are typically overlain by Al-phyllosilicates. The purpose of this study is to map and characterize an additional series of surface to near-surface phyllosilicate-bearing outcrops exposed on the high-standing plateau region of West Margaritifer Terra (WMT), centrally located between the exposures near Valles Marineris and in Mawrth Vallis/Arabia Terra (Fig 1). This geographic proximity suggests a similar formation mechanism is possible, which would support the idea that a large, nearly contiguous area of the Noachian/Hesperian crust was subjected to an active and sustained hydrologic cycle [10]. However, the WMT region has also been subjected to significant fluvial erosion and flooding events, providing other reasonable pathways for phyllosilicate formation, transport, and/or re-deposition. Phyllosilicate formation via diagenetic and/or hydrothermal activity has also been deduced for many other areas of Mars; therefore, we also consider these scenarios in our evaluation.

Datasets and Methodology: We used multiple remote sensing datasets to characterize the WMT phyllosilicates. Outcrops were first delineated in an ArcGIS framework at ~1:250K scale using Compact Reconnaissance Imaging Spectrometer for Mars (CRISM) mapping data (180 m/pix) in conjunction with several base datasets. CRISM mapping data were processed to remove photometric and atmospheric effects as well as instrument residuals prior to the calculation of summary parameters (e.g., band depths) that were then mosiacked in 5°x5° tiles. All or part of 16 tiles cover the study area, which extends from 325°E to 345°E, 0°N to -15°N. For this effort, D2300 was the most commonly utilized parameter, typically indicative of Fe/Mg phyllosilicate which displays distinct absorptions at 1.4, 1.9 and 2.3 μm. High spatial and spectral resolution CRISM targeted observations (~20/40 m/pix) were processed as Map-projected Targeted Reduced Data Records (MTRDRs) [11], comprising a suite of fully corrected spectral data, summary parameter cubes [12], and visual products that facilitate spectral analysis. Ninety-six MTRDR images were systematically analyzed and used to verify mapping results from the mapping data as well as to catalog particular mineral species. Thermal Emission Imaging System (THEMIS) daytime IR controlled mosaics [13] and qualitative thermal inertia [14], Mars Orbiter Laser Altimeter (MOLA) 128 pix/deg gridded topography, and select High Resolution Stereo Camera (HRSC) DTMs served as basemaps for unit mapping. Tiled mosaics of Context Imager (CTX) data processed through the Projection on the Web (POW) utility [15] and High Resolution Imaging Science Experiment (HiRISE) data (including color and DTMs) were used to examine morphologic characteristics. To explore the relationship of the outcrops to fluvial activity, we also compared outcrops to channel and basin locations, which included valley networks, outflow channels, and broad channels that cross over the plateau and/or connect to other channels or chaos terrains.

Results: Phyllosilicate outcrops are distributed throughout the Noachian plateau region (Fig. 1), unconstrained by the younger outflow channels, chasma, or chaos terrains and with no apparent elevation threshold. Outcrops exhibit higher thermal inertia than surroundings, signifying a relatively consolidated nature, and appear light-toned with polygonal fracturing. Three types of exposures all indicate shallow emplacement: a) surficial outcrops on plains, b) in fracture/chaos walls, and c) in crater rims and ejecta. Outcrops are consistently cross-cut by Hesperian-aged chaos and fractures.

Where exposed vertically, deposits can have variable thickness on the order of a few to several 10s of meters, sometimes with subparallel internal layering. Upper contacts tend to be relatively sharp, but determining the nature of the lower contact has proved elusive because of mass wasting. Superposed material, where present, is spectrally neutral to vaguely mafic. HiRISE color data suggests some vertical compositional variation with reddish light-toned material overlain by blueish material, but so far no spectral differences have been identified. Instead, hyperspectral data consistently show the phyllosilicates to be dominated by Mg-smectite (e.g., saponite), which is similar to phyllosilicates identified to the west and southwest [3-5]. In contrast to some of those outcrops, however, no Al-phyllosilicates are observed to overly the Fe/Mg smec-

tite. Other mineral species (zeolite, chloride) are observed in only a few instances. Low-calcium pyroxene is fairly common on the plateaus, consistent with other Noachian-aged highland terrains.

Evaluating Emplacement Mechanisms: Our mapping results and observations can be compared to expected characteristics of the 4 formation mechanisms (fluviolacustrine, pedogenic, diagenetic, or hydrothermal) to determine the most likely scenario. The region-wide occurrence and spectral homogeneity of Mg-smectite disfavors emplacement by a hydrothermal process, where zonation or a regional gradient would be expected. The shallowness of the outcrops and lack of significant vertical variability similarly contradicts burial diagenesis, although deposition of an easily-altered volcanic ash layer with subsequent alteration by ground water could be feasible. The paucity of Al-phyllosilicate does not necessarily rule out pedogenic weathering; however, it does suggest either an immature pedogenic profile and/or mechanical stripping of the uppermost layer(s) where Al-phyllosilicate would be concentrated. Fluviolacustrine deposition likewise cannot fully explain the spatial distribution of outcrops, although the location of some prominent outcrops alongside channels or at basin margins may suggest at least some of the outcrops could have been emplaced in low energy aqueous environments [e.g., 16]. Given the spectral uniformity, one scenario could be that the phyllosilicates were 1) initially formed as a result of pedogenic weathering or shallow groundwater diagenesis, 2) partially mobilized by aqueous activity and redeposited in local topographic lows, 3) sometimes buried by other sediment or volcanic flows, and if so, 4) later exposed via impact, chaos/fracture formation, or surface weathering.

Conclusion and Future Work: Mapping and characterization of phyllosilicate outcrops in WMT reveals that a continuation of the regional layer observed to the west along the walls and plains surrounding Valles Marineris and in NW Noachis Terra is feasible, but significant fluviolacustrine activity likely played an important role in redistributing and perhaps concentrating the clay-bearing material. Additional morphologic characterization using high resolution CTX and HiRISE DTMs will allow us to evaluate regional variation in deposit thickness, dip, and internal structures to further constrain how these altered materials arrived at their present location and what clues they may harbor for further understanding Mars' Noachian climate history.

References: [1] Noe Dobrea, E. Z., et al. (2010), *JGR, 115(E00D19)*. [2] Poulet, F., et al. (2005), *Nature, 438(7068)*. [3] Le Diet, L. et al. (2012), *JGR, 117(E00J05)*. [4] Buczkowski, D. L., et al. (2010), *41st LPSC*, Abstract #1458. [5] Loizeau et al. (2016) *47th LPSC*, Abstract #2280. [6] McKeown, N. K., et al. (2009), *JGR, 114(E00D10)*. [7] Wiseman, S. M., et al. (2010), *JGR, 115(E00D18)*. [8] Wiseman, S. M., et al. (2008), *GRL, 35(L19204)*. [9] Mustard, J. F. et al. (2009), *JGR, 114(E00D12)*. [10] Andrews-Hanna, J. C., and R. J. Phillips (2007), *JGR, 112(E08001)*. [11] Seelos, F. P. et al., (2014) *USGS Open File Report 2014-1056*. [12] Viviano-Beck, C. E., et al., (2014) *JGR, 119,* 1403–1431. [13] Fergason, R. L., et al. (2013), *44th LPSC*, Abstract #1642. [14] Fergason, R. L., et al. (2006), *JGR, 111(E12004)*. [15] Hare, T. M., et al. (2014), *45th LPSC*, Abstract #2487. [16] Salvatore, M. R., et al. (2015) *JGR, 121* 273-295.

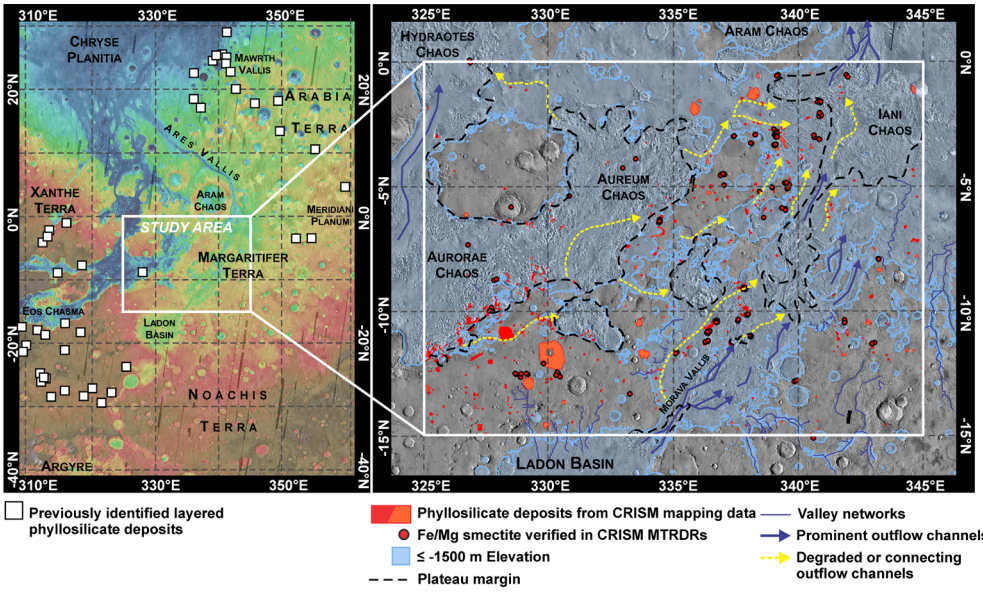

Figure 1. Regional context and mapping results. Left panel shows regional MOLA elevation and selected previous identifications of phyllosilicates [1-8]. Right panel shows phyllosilicate outcrops mapped in this study overlain on THEMIS daytime IR mosaic with fluvial features highlighted for comparison. (For simplicity, other identified minerals are not shown.) Phyllosilicate outcrops occur both above and below the -1500 m elevation contour (blue shading), which seems to correlate fairly well to the boundary of many topographic basins, channel margins, and valley network terminations.